International Conference on Nuclear Data for Science and Technology 2007
DOI: 10.1051/ndata:07563

^{6}Li(n,t)α angular distribution measurements for $0.2 < E_n < 10$ MeV at LANSCE/WNR

M. Devlin[1,a], T.N. Taddeucci[1], G.M. Hale[2], and R.C. Haight[1]

[1] LANSCE-NS, Los Alamos National Laboratory, Los Alamos, NM 87545, USA
[2] T-16, Los Alamos National Laboratory, Los Alamos, NM 87545, USA

Abstract. Measured angular distributions of tritons following the ^{6}Li(n,t)α reaction are reported for incident neutron energies between 0.19 to >10 MeV. The neutrons were produced by spallation at the WNR facility at the Los Alamos Neutron Science CEnter (LANSCE), with the incident neutron energy determined by the time-of-flight method. The data were taken with four E-ΔE telescopes at eight laboratory angles. These data have been incorporated into an R-matrix analysis of the ^{6}Li(n,t)α reaction. The current measurements are compared to previous data, and the implications of these data to the current R-matrix analysis are discussed.

1 Introduction

The exothermic ^{6}Li(n,α)t reaction (Q = 4.78 MeV) is widely used in neutron detection and other applications, and as such its cross section is well measured and is in fact considered a standard at low neutron energies. However, in the few MeV incident-neutron energy range, despite a number of measurements, this cross section is considered to be uncertain by as much as 20%. As a result of this situation, a series of measurements of both the reaction cross section and the angular distribution of the products has been begun using a spallation neutron spectrum at LANSCE.

In addition, measurements on the same reaction at discrete incident neutron energies from 1.05 to 4.42 MeV have been recently been reported [1–3]. These measurements made use of the Peking University Van de Graaff accelerator and the T(p,n) reaction to produce neutrons, and the gridded ionization chamber (GIC) technique to detect the reaction products [4]. The GIC technique simultaneously determines the cross section and the product angular distributions. These measurements are generally consistent with the prior data – though with a few notable exceptions in the angular distributions above 3 MeV, and they agree with some evaluations better than with others. For example, these data suggest that in the 1 to 2.5 MeV energy range that the ENDF/B-VI evaluation somewhat overestimates the reaction cross section. Such descrepancies raise concerns that the current understanding of this reaction is inadequate.

Recent theoretical analyses using the R-matrix [5] and Refined Resonant Group Model (RRGM) [6] have been reported. The authors suggest that uncertainties about the position of the large $5/2^-$ resonance near 240 keV, and the positions and nature of the apparent smaller resonance structures near 2 MeV, give rise to too large uncertainties in the fitted cross section of this reaction in the few MeV region. As a result, new measurements were again suggested as a way to resolve these issues.

Differential cross section measurements provide information on the nature and strength of resonances in the compound system, in this case ^{7}Li. In this paper we address these issues by presenting new triton angular distribution measurements performed at LANSCE, and compare them with both prior data and R-matrix models of the ^{6}Li(n,α)t reaction.

2 Description of the experiment

The neutron beam was produced by spallation following the bombardment of a tungsten target by 800 MeV protons at the Weapons Neutron Research facility (WNR) [7] of the Los Alamos Neutron Science CEnter (LANSCE). The experiments were conducted using the "n,z" scattering chamber located at 15.1 m on a flight path at 30 degrees relative to the proton beam. The beam structure consisted of micropulses of protons separated by 1.8 or 3.6 μs. The neutron beam was monitored with a ^{235}U fission chamber [8]. The incident neutron energy was determined using the time-of-flight technique, corrected for the time-of-flight of the subsequent reaction product detected.

The reaction products were detected in four three-stage particle telescopes, which were variously positioned at eight scattering angles during the experiment. Each telescope consisted of a gas ΔE detector, followed by a Si detector, and finally by a CsI detector. The gas used in the ΔE detectors was approximately 20 torr of P-10 gas (10% methane in 90% argon) and this was provided by filling the entire scattering chamber. The Si detectors were manufactured by AMETEK (ORTEC) and were 500 μm thick. The CsI detectors were not used in the data analysis for this experiment, as the reaction products of interest were stopped in the Si detectors. Further details of this apparatus can be found in S. Grimes et al. [9]. Figure 1 shows a picture of the inside of the scattering chamber, with the target ladder lowered out of the beam path. In addition to the telescopes, various materials are used to shield the detectors are shown.

The targets were composed of ^{6}LiF, with the Li enriched to 95.5% ^{6}Li, evaporated onto a thin mylar backing. Typical target thicknesses were 1.0 mg/cm^2 LiF on 0.84 mg/cm^2 mylar. The neutron beam spot was approximately 0.6" diameter, and the targets were 2" in diameter. The target and backing

[a] Presenting author, e-mail: devlin@lanl.gov

thicknesses and uniformities were determined by α particle energy loss measurements and analysis using the code SRIM [10]. Since this procedure only indirectly determines the ^{6}Li content of the targets, a further direct measurement of this is planned. Until it is complete, we are scaling upward by a factor of 1.4 the measured differential cross sections (for all angles and energies) in order to agree on average with the current R-matrix fit of the reaction cross section. It is thought that the need for this factor arises from an incomplete description of the chemical content of the targets. In either event, until a direct measurement of the ^{6}Li content of the targets is made, these measurements should be considered only as angular distribution measurements. The relative efficiency of the detector telescopes at different angles was determined with a ^{229}Th source placed in the target position, and the uncertainties in these efficiencies are estimated to be $+/-2\%$.

The ΔE vs. E (from the Si detectors) data were used to distinguish between alpha particles and tritons from the ^{6}Li(n,α)t reaction; despite the fact that the resolution of the telescopes was not sufficient to distinguish tritons from protons, the excess energy of the tritons from the ^{6}Li(n,α)t reaction cleanly separated them from other hydrogen isotopes created in the target. This is seen clearly in figure 2, which shows the ungated and α-gated Si energy versus time-of-flight (TOF) spectra for data taken with a micropulse spacing of 1.8 μs. At this micropulse spacing, neutrons below ~300 keV arrive at the target after neutrons from the next micropulse. As a result, a micropulse spacing of 3.6 μs was used to collect data below this energy.

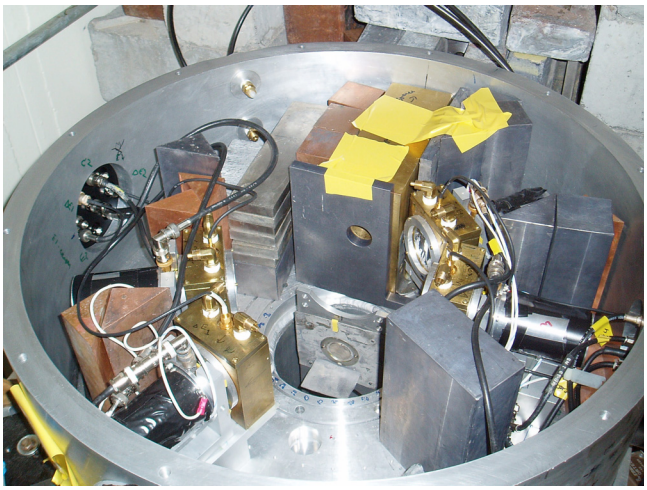

Fig. 1. The scattering chamber used for these measurements.

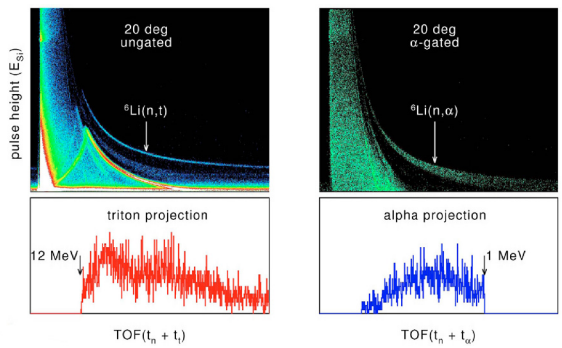

Fig. 2. Si detector energy versus time-of-flight (TOF) spectra for a WNR spacing of 1.8 μs (see text) at a laboratory angle of 20 degrees. Both raw (left) and α gated (right) spectra clearly show the reaction products from the ^{6}Li(n,α)t reaction.

3 Results and discussion

Data were taken at eight laboratory angles: 20, 30, 45, 60, 75, 90, 120 and 135 degrees. The resulting (scaled) triton differential cross sections are shown in figures 3 and 4 for these angles. These are compared to recent R-matrix fits to the available nuclear data for this system. These data, and the corresponding α particle angular distribution data taken at 5 angles in the same experiments (not shown here), were also included in the R-matrix fit shown.

These new triton angular distribution data generally agree very well with prior data and the R-matrix expectations (even before these data were included in the fits). The large resonance at 240 keV is well described, consistent with prior measurements. For incident neutrons in the 2–4 MeV, however, there are some notable differences.

In figures 5 and 6 we show angular distributions at eight incident neutron energies in the energy range of 1.1 to

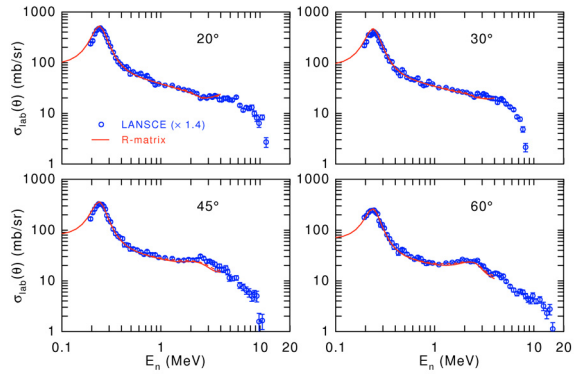

Fig. 3. Measured laboratory differential cross sections for tritons at four angles as a function of incident neutron energy. The solid line is an R-matrix fit, including the new data.

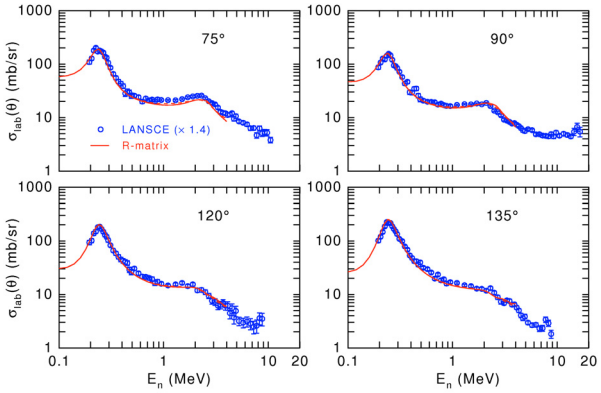

Fig. 4. Measured laboratory differential cross sections for tritons at four additional angles as a function of incident neutron energy.

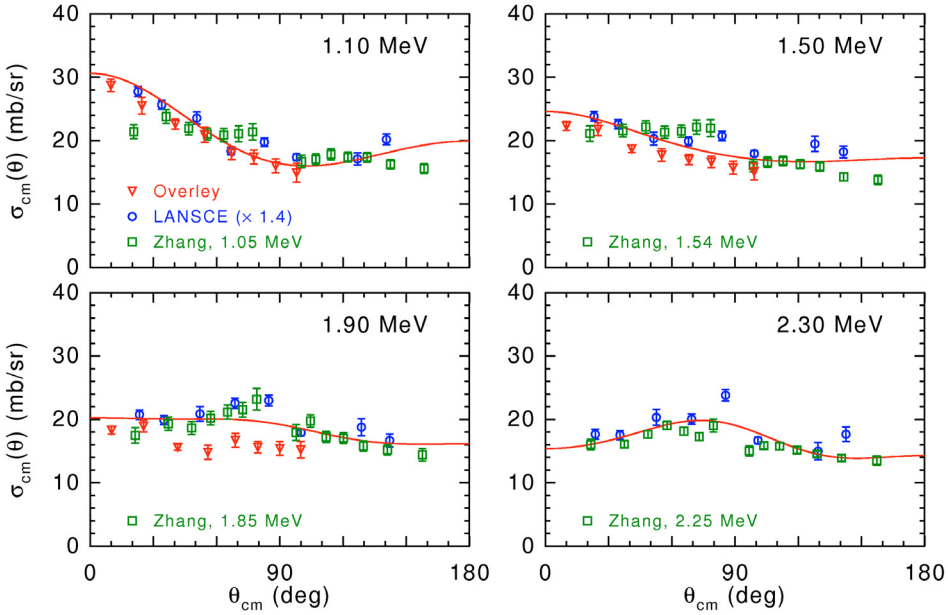

Fig. 5. Measured differential cross sections for tritons (circles) as a function of center-of-mass angles, at four incident neutron energies. The incident neutron energy labels (upper right of each panel) correspond to the midpoint of 200 keV wide energy for the LANSCE data. Data from J.C. Overley et al. [11] (triangles) at the same energies, and G. Zhang et al. [1–4] (squares) at the labeled energies, are shown for comparison. The line is the most recent R-matrix fit, which includes the new LANSCE data.

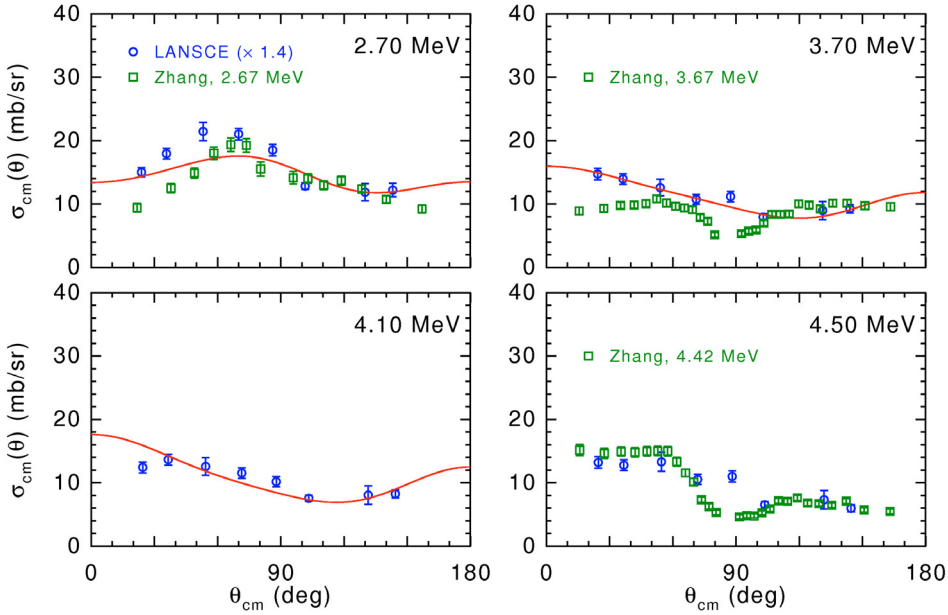

Fig. 6. Measured differential cross sections for tritons as a function of center-of-mass angles, at four additional incident neutron energies. See figure 5 caption for explanation.

4.5 MeV. The incident neutron energy labels in each panel correspond to the midpoint of 200 keV-wide energy bins for the LANSCE data. Where available, data from J.C. Overley et al. [11] (triangles) at the same energies, and recent data from G. Zhang et al. [1–4] (squares) at the labeled energies, are shown for comparison. The Overley data sets are shown as representative of a number of older measurements, and the recent Zhang data are shown for comparison. The line is the most recent R-matrix fit, which includes the new WNR data; note that this fit does not include the Zhang data.

For neutron energies between 1.1 and 2.3 MeV (fig. 5), the new LANSCE data agree very well with the prior data, with somewhat of an exception in the shape of the Overley [11] data at 1.9 MeV. For incident neutron energies of 2.7, 3.7 and 4.5 MeV, significant differences between the current data and that of Zhang can be seen in the figures. At 2.7 and

3.7 MeV, the LANSCE data do not agree with the shape of the angular distributions reported by Zhang [2,4] at forward angles. And we do not support the apparent "dip" in the angular distributions at 90 degrees in the 3.67 and 4.42 MeV [1,4]. In addition, the new LANSCE data suggest that the prior R-matrix fit in the 2–4 MeV region can be improved. Above 4 MeV, the R-matrix calculations are not available, so no comparison can be made. The data however extend to 10 MeV and above at some angles.

4 Conclusion

We have used the LANSCE/WNR spallation source to measure the angular distribution of α particles and tritons following the ^{6}Li(n,α)t reaction. As can be seen in figures 3 and 4, the data reported on here offers a very complete picture of the angular distribution of tritons following this reaction from below 200 keV to above 10 MeV. These data are being incorporated into a current R-matrix model. Separately, we are also measuring the ^{6}Li(n,α)t reaction cross section at LANSCE in the same incident neutron energy range to better accuracy, with a goal of achieving a 5% uncertainty in this important cross section in the few MeV region.

This work is being supported by the US Department of Energy under contract DE-AC52-06NA25396. The assistance of Ron Snow in making the targets and John O'Donnell in data acquisition are gratefully acknowledged.

References

1. Guohui Zhang, Guoyou Tang, Jinxiang Chen, Zhaomin Shi, Guangzhi Liu, Xuemei Zhang, Zemin Chen, Yu.M. Gledenov, M. Sedysheva, G. Khuukhenkhuu, Nucl. Sci. Eng. **134**, 312 (2000).
2. Guohui Zhang, Guoyou Tang, Jinxiang Chen, Zhaomin Shi, Zemin Chen, Yu.M. Gledenov, M. Sedysheva, G. Khuukhenkhuu, Nucl. Sci. Eng. **143**, 86 (2003).
3. Guohui Zhang, Rongtai Cao, Jinxiang Chen, Guoyou Tang, Yu.M. Gledenov, M. Sedysheva, G. Khuukhenkhuu, Nucl. Sci. Eng. **153**, 41 (2006).
4. Guohui Zhang, Jinxiang Chen, Guoyou Tang, Yu.M. Gledenov, M. Sedysheva, G. Khuukhenkhuu, Nucl. Instrum. Meth. in Phys. Res. A **566**, 615 (2006).
5. Gerald M. Hale, Hartmut M. Hofmann, in *International Conference on Nuclear Data for Science and Technology*, edited by R.C. Haight, M.B. Chadwick, T. Kawano, P. Talou, AIP Conference Proceedings **769**, 75 (2005).
6. Zhenpeng Chen, Yeying Sun, Rui Zhang, Tingjin Liu, abstract in *Nuclear Data 2004 Proceedings supplement*.
7. P. Lisowski et al., Nucl. Sci. Eng. **106**, 208 (1990).
8. S.A. Wender et al., Nucl. Instrum. Meth. Phys. Res. A **336**, 226 (1993).
9. S.M. Grimes et al., Nucl. Sci. Eng. **124**, 271 (1996).
10. James F. Ziegler, *SRIM – The Stopping and Range of Ions in Matter*, version SRIM-2006, computer code, available from http://www.srim.org/#SRIM.
11. J.C. Overley, R.M. Sealock, D.H. Ehlers, Nucl. Phys. A **221**, 573 (1974).